Numerical analysis of fractional viscoelastic column based on shifted Chebyshev wavelet function

Jiawei Cao, Yiming Chen, Yuanhui Wang, Gang Cheng, Thierry Barrière, Lei Wang

Version of Record: https://www.sciencedirect.com/science/article/pii/S0307904X2030576X
Manuscript_000cb3aef8b3010f26fa3d50eaed4900

Numerical analysis of fractional viscoelastic column based on shifted Chebyshev wavelet function

Jiawei Cao[a], Yiming Chen[a,b,*], Yuanhui Wang[a], Gang Cheng[c], Thierry Barrière[b], Lei Wang[a]

[a] *College of Sciences, Yanshan University, 066004 Qinghuangdao, Hebei, China*
[b] *Univ. Bourgogne Franche-Comté, FEMTO-ST Institute, CNRS/ENSMM/UTBM, Department of Applied Mechanics, 25000 Besançon, France*
[c] *INSA Centre Val de Loire, Univ. Tours, Univ. Orléans, LaMé, 3 rue de la chocolaterie, CS 23410, 41034 Blois, France*

Abstract

An innovative numerical procedure for solving the viscoelastic column problem based on fractional rheological models, directly in the time domain, is investigated. Firstly, the governing equation is established according to the fractional constitutive relation. Secondly, the resulting equation is transformed into algebraic equation and solved by using the shifted Chebyshev wavelet function. Furthermore, the convergence analysis and the retained numerical benchmarks are carried out to validate the performance of the proposed method. A small value of the absolute error between numerical and accurate solution is obtained. Finally, the dynamic analysis of viscoelastic beam-column problems is investigated with different cross-section shape (circular and square) under various loading conditions (axial compressive force and harmonic load). The displacement, strain and stress of the viscoelastic column at different time and position are determined. The deformation and stress of the viscoelastic column of different materials under the same loading condition are compared. The results in the paper show the highly accuracy and efficiency of the proposed numerical algorithm in the dynamical stability analysis of the viscoelastic column.

Keywords: Fractional constitutive model, Viscoelastic column, Shifted Chebyshev wavelet function, Convergence analysis, Numerical solution

*Corresponding author
Email address: chenym@ysu.edu.cn (Yiming Chen)

1. Introduction

Non-integer or fractional viscoelastic constitutive models attract more and more attention [1]. These models are widely used to describe the viscoelastic behaviour of materials with the development of fractional order differential operators. The memory properties of viscoelastic materials are described better with these operators. Xu et al. [2] used the wave method to analyze the structure of fractional-order viscoelastic beams, and discussed the effect of fractional order on the structure during the analysis. Mendiguren et al. [3] proposed a one-dimensional fractional-order elastoplastic model. They analyzed the special cases of first, second, and third terms, which fitted with experimental data, and compared with the classic Hollomon and Ramberg-Osgood models. Sherief et al. [4] studied the variable thermal conductivity of material with half-space method in the context of fractional-order thermoelasticity theory. The effect of fractional derivative parameters on the behaviour of the solution was also investigated. Therefore, fractional order is more suitable than integer order for solving problems in real life. Liaskos et al. [5] derived the implicit analytical solutions for a nonlinear fractional governing equation of viscoelastic Euler-Bernoulli beam. Lin et al. [6] established the governing equations related to the left and right Riemann-Liouville fractional derivatives. A comprehensive study was effectuated on the flow and heat transfer of the space fractional boundary layer with a variable thickness stretching sheet. Their results showed considerable importance of fractional calculus in the numerical modelling of viscoelastic behaviour of materials.

The column structure may exhibit complex dynamic behaviour due to different dynamic loads and working environments in building structures and aircraft interior products. The study focus on the dynamic stability of viscoelastic column is paid much attention [7]. In recent years, the analysis of the stability of this structure using Lyapunov functions is well developed [8,9].

Viscoelastic materials are of great significance in vibration system design [10]. Viscoelastic damping exhibited in glassy materials. Yang et al. [11] proposed an adaptive segmentation algorithm for time to describe the static and dynamic stability of the viscoelastic column. Deng et al. [12] used the stochastic averaging method to investigate the stability of viscoelastic

beam-column under random axial loading. A new set of mean variables was proposed to approximate the response of the dynamical system. The Lyapunov exponent was retained to resolve the eigenvalue problem. A high-order stochastic averaging method was applied to investigate the stochastic stability of a fractional order viscoelastic column with axially random force loading [13]. Amit et al. [14] studied the non-linear flexural-torsional vibration and instability analysis of the thin-walled column with different cross-sections under cyclic axial loading. The effect of eccentricity, cross-sectional shape and boundary condition on the response of the frequency amplitude and instability region was analysed. Floris et al. [15] examined the stability of a hinged-hinged viscoelastic column under random axial forces of Gaussian white noise. The response of the differential equation was obtained by using Itô's differential law. The necessary and sufficient numerical conditions for stability of the viscoelastic column were that the coefficient matrix were negative real eigenvalues and complex eigenvalues with negative real part. Leung et al. [16] used the Runge-Kutta method to research the bifurcation behaviour of viscoelastic column at different fractional orders and material properties. The stability of viscoelastic column was illustrated by the curves of amplitude and frequency response. Zhang et al. [17] developed a fractional nonlinear viscoelastic model to describe the large deformation of biomaterials. The fractional viscoelastic constitutive model was integrated in a finite element framework. The proposed method showed high computational efficiency and better convergence rate.

The dynamic analysis of viscoelastic column is not limited to the establishment of the material behaviour equations, but also to solving the fractional differential equations with an efficient numerical algorithm. The conventional approaches are based on the multi-scale [18], galerkin method [19], finite element method [20]. Betancur-Herrera and Munoz-Galeano [21] proposed an innovative numerical method to solve the fractional derivative equations with Riemann-Liouville's or Caputo's form. The main contribution of the method was transforming the fractional derivatives to recurrence equations, which allowed to solve the fractional equations as a system of algebraic equations. Chen et al. [22] proposed a correction method to obtain the numerical solutions of the fractional differential equations. The improved Lubich's method with few correction terms demonstrated high accuracy compared with other presented methods. Many time domain problems are converted into frequency-domain by using Laplace transform. The solution in the time domain is determined by using the inverse of Laplace

transform in the frequency-domain. The inconvenient of this method is the complexity of Laplace transform and its inverse transform. Qi and Guo [23] applied the fractional calculus approach to find the numerical solutions of an initial-boundary value problem. The Laplace transform was used to present the solution under series forms of H-function to facilitate the numerical computation. The wavelet basis function is proposed to solve fractional differential equations directly in time domain. Its advantages are high-accuracy, fewer iterations and less computation time [24]. Legendre [25], Bernstein [26,27] and Chebyshev polynomials [28-30] are often employed to construct wavelet algorithms. Chen et al. [31] employed wavelet method for solving the non-linear fractional differential equations. The absolute error between the numerical and the algebraic solution was estimated. The shifted Chebyshev polynomials with variable coefficients was proposed to solve the generalized fractional pantograph equations by Wang et al. [32]. Yu et al. [33] applied Quasi-Legendre polynomials to solve the governing equation of the viscoelastic Euler-Bernoulli beam. Hassani et al. [34] used a novel class of basis functions based on the shifted Chebyshev polynomials to solve the nonlinear variable order fractional derivative equations. The accuracy and efficiency of the method was confirmed by the convergence analysis and several numerical examples.

Although many researches on the stability of viscoelastic column in various aspects were effectuated, less method has been proposed to solve directly the displacement, stress and strain of viscoelastic column with different materials in the time domain. In this paper, the shifted Chebyshev wavelet function is proposed to perform the dynamic analysis of viscoelastic column directly in the time domain. The material properties are described with a fractional viscoelastic model. The governing equation of column with this fractional viscoelastic model is established. An efficient numerical algorithm based on the shifted Chebyshev wavelet functions is proposed to solve the governing equations. The performance and efficiency of the developed algorithm are investigated. The numerical solutions concerning the displacement, stress and strain of the column have been obtained under axial compressive force and harmonic load conditions. The displacement solutions of viscoelastic columns with different cross-sections and materials under the same load are compared. It provides theoretical basis and numerical approach for the application of viscoelastic materials in engineering.

This paper is structured as follows, section 2 is the introduction of fractional order and viscoelastic material parameters. Section 3 shows

the governing equation of the viscoelastic column. Section 4 presents the proposed algorithm. The convergence of the algorithm is analyzed in section 5. The displacement, strain and stress of the viscoelastic column with different materials under different loading conditions are obtained and compared in section 6. The research work is concluded in section 7.

2. Preliminary

2.1. Definition of fractional derivative

In fractional calculus, the different operators called Riemann-Liouville, Caputo and Grünwald-Letnikov operators are respectively defined in [35], [36] and [37]. The definition and properties of the fractional derivatives of Caputo are introduced as follows.

Definition 1 *Fractional Caputo derivative*

$$ {}^{c}D_{t}^{\alpha} f(t) = \begin{cases} \frac{d^{m} f(t)}{dt^{m}}, \alpha = m \in N^{+} \\ \frac{1}{\Gamma(m-\alpha)} \int_{a}^{t} \frac{f^{(m)}(\tau)}{(t-\tau)^{\alpha-m+1}} d\tau, 0 \leq m-1 < \alpha < m \end{cases} \tag{1} $$

where $0 < \alpha < 1$ is fractional derivative order, ${}^{c}D_{t}^{\alpha}$ is Caputo fractional derivative operator, $f(t)$ is a continuous function, m is positive integer, $\Gamma(\cdot)$ is Gamma function, and $\Gamma(z) = \int_{0}^{\infty} e^{-t} t^{z-1} dt$.

Based on the above definition, the following equations are obtained

$$ {}^{c}D_{t}^{\alpha} t^{m} = \begin{cases} 0, m \in N_0 \, and \, m < \alpha \\ \frac{\Gamma(m+1)}{\Gamma(m+1-\alpha)} t^{m-\alpha}, m \in N_0 \, and \, m \geq \alpha \; or \; m \notin N_0 \, and \, m > \alpha \end{cases} \tag{2} $$

The Caputo fractional derivative of constant is zero.

$$ {}^{c}D_{t}^{\alpha} C = 0 \tag{3} $$

where C is constant.

The Caputo fractional derivative is a linear operator.

$$ {}^{c}D_{t}^{\alpha}(C(f(x))) = C {}^{c}D_{t}^{\alpha} f(x) \tag{4} $$

2.2. Constitutive equation of linear viscoelasticity

Many materials used in mechanical engineering exhibit elastic and viscous behaviours simultaneously. Lots of physical models have been proposed to describe their viscoelastic characteristic. This viscoelastic relationship between stress and strain could be described more completely and accurately by the fractional order constitutive equation compared to integer order constitutive equation.

The linear viscoelastic properties of the materials can be modelled by different combinations of elastic and viscous elements. The fractional constitutive viscoelastic models, such as Four-parameter Zener model (FZM) [38], Poynting-Thomson model (PTM) [39], Fractional Maxwell model (FMM) [40] and Fractional Kelvin-Voigt model (FKVM) [41] have been used to describe the viscoelasticity of the materials. Liu et al. [42] employed the time fractional Maxwell constitutive equation to investigate the boundary layer flow. The fractional order operator exhibits better memory characteristic in describing the flow in a highly non-homogeneous transport process. The classical Kelvin-Voigt model is represented by a purely viscous dashpot and a purely elastic string connected in parallel. In fractional Kelvin-Voigt model, the purely viscous dashpot is replaced by a fractional element, as shown in Eq. (5). When the fractional order α is equal to 1, the model reduces to the classical Kelvin-Voigt model. The FKVM requires fewer parameters to be identified by the experimental tests. Farno et al. [43] showed that FKVM can better explain the performance of viscoelastic materials than classic Kelvin-Voigt model. In this paper, FKVM is retained to describe the constitutive relationship between stress and strain of viscoelastic material. FKVM is represented in Figure. 1 and its constitutive equation is as follows:

$$\sigma(x,t) = [E_0 + \eta \cdot {}^{c}D_t^{\alpha}]\,\varepsilon(x,t) \tag{5}$$

where E_0 is elastic modulus, η is viscosity, $\sigma(x,t)$ is stress, $\varepsilon(x,t)$ is strain.

2.3. FKVM parameters

The material physical properties can be characterized by the dynamic mechanical analysis. The viscoelastic parameters in the fractional behaviour law, such as fractional order, elastic modulus, can be identified according to the regression analysis. Leung et al. [16] found that the stability domain of the viscoelastic column increases with time-delays when $\alpha = 0.8, \eta = 0.05$

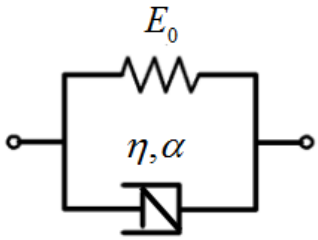

Figure 1: Schematic representation of FKVM.

by comparing the results with different values of α and η. The numerical results obtained by the direct integration based on the Runge-Kutta 4^{th} order method are approximately equivalent to the analytical solution. The description of geometrical and material properties [44,45] are shown in Table. 1.

Table 1: Description of geometrical and material properties of the viscoelastic column.

	l(m)	ρ(kg/m^3)	$\beta_0(1)$	E_0(MPa)
Metal	5	7750	600	21
Concrete	5	4000	600	22680
Polymer	5	1300	600	3162.4

3. Development of fractional governing equation of viscoelastic column

When the axial compressive load $F(t)$ is applied on the viscoelastic column, the transverse displacement appears, as shown in Figure. 2, where the transverse displacement is noted as $v(x,t)$, x and z are axial and transverse coordinate respectively.

The fractional dynamic equation of the column [13] is given as

$$\frac{\partial^2 M(x,t)}{\partial x^2} = \rho A \frac{\partial^2 v(x,t)}{\partial t^2} + \beta_0 \frac{\partial v(x,t)}{\partial t} + F(t) \frac{\partial^2 v(x,t)}{\partial x^2}, \tag{6}$$

where density is ρ, damping coefficient is β_0, cross-sectional area is A, and the bending moment is $M(x,t)$.

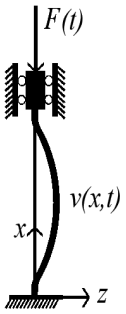

Figure 2: The displacement of viscoelastic column.

The bending moment is

$$M(x,t) = \int_A \sigma(x,t)\, z dA. \tag{7}$$

When the column exhibits the small deformation, the strain of the column is expressed as

$$\varepsilon(x,t) = -\frac{\partial^2 v(x,t)}{\partial x^2} z \tag{8}$$

Substituting Eq. (5) into Eq. (7), it can get

$$M(x,t) = \int_A [E_0 + \eta \cdot {}^c D_t^\alpha] \varepsilon(x,t)\, z dA \tag{9}$$

Based on Eq. (8) and (9), the bending moment of viscoelastic column is

$$M(x,t) = -E_0 I \frac{\partial^2 v(x,t)}{\partial x^2} - \eta I^c D_t^\alpha \frac{\partial^2 v(x,t)}{\partial x^2}, \tag{10}$$

where $I = \int_A z^2 dA$ is the moment of inertia.

Then

$$\frac{\partial^2 M(x,t)}{\partial x^2} = -E_0 I \frac{\partial^4 v(x,t)}{\partial x^4} - \eta I^c D_t^\alpha \frac{\partial^4 v(x,t)}{\partial x^4} \tag{11}$$

Therefore, the fractional governing equation of viscoelastic column is obtained as

$$\rho A \frac{\partial^2 v(x,t)}{\partial t^2} + \beta_0 \frac{\partial v(x,t)}{\partial t} + E_0 I \frac{\partial^4 v(x,t)}{\partial x^4} + \eta I^c D_t^\alpha \frac{\partial^4 v(x,t)}{\partial x^4} + F(t) \frac{\partial^2 v(x,t)}{\partial x^2} = 0. \tag{12}$$

4. Shifted Chebyshev wavelet function algorithm

A numerical algorithm is proposed to obtain the solutions of the fractional governing equations. The operator matrices of integer and fractional order are deduced according to the shifted Chebyshev wavelet function.

4.1. Shifted Chebyshev wavelet function

The Chebyshev polynomials defined above [-1, 1] are derived. The expression of Chebyshev polynomials is obtained by the following recursive formula

$$T_{i+1}(z) = 2zT_i(z) - T_{i-1}(z), i = 1, 2\cdots \tag{13}$$

where T is a function expression and $T_0(z) = 1,\ \ T_1(z) = z$.

The conversion variable $z = \frac{2x}{L} - 1$ is introduced to obtain the shifted Chebyshev wavelet function in the interval of $[0,\ L]$.

$$T_{i+1}\left(\frac{2x}{L} - 1\right) = 2\left(\frac{2x}{L} - 1\right)T_i\left(\frac{2x}{L} - 1\right) - T_{i-1}\left(\frac{2x}{L} - 1\right), i = 1, 2\cdots \tag{14}$$

Let $T_i\left(\frac{2x}{L} - 1\right) = G_i(x)$, the shifted Chebyshev wavelet function becomes:

$$G_{i+1}(x) = 2\left(\frac{2x}{L} - 1\right)G_i(x) - G_{i-1}(x), i = 1, 2\cdots \tag{15}$$

where $G_0(x) = 1, G_1(x) = \frac{2x}{L} - 1$.

The specific expression of the shifted Chebyshev wavelet function of order i is

$$G_i(x) = i\sum_{k=0}^{i}(-1)^{i-k}\frac{(i+k-1)!2^{2k}}{(i-k)!(2k)!L^k}x^k, i = 1, 2\cdots \tag{16}$$

where $G_i(0) = (-1)^i, G_i(L) = 1$.

The shifted Chebyshev wavelet function satisfies the following orthogonality relation

$$\int_0^L G_j(x)\,G_k(x)\,v_L(x)dx = h_k \tag{17}$$

where $v_L(x) = \frac{1}{\sqrt{Lx-x^2}}, h_k = \begin{cases} \frac{b_k}{2}\pi, k = j \\ 0, k \neq j \end{cases}, b_0 = 2, b_k = 1, k \geq 1.$

Then a series of shifted Chebyshev wavelet function matrix $\Phi(x)$ can be written as

$$\Phi(x) = [G_0(x), G_1(x), \cdots, G_n(x)]^T = A_n Z(x) \tag{18}$$

where $Z(x) = [1, x, \cdots, x^n]^T$,

$\mathrm{A}_n = [p_{ij}]_{i,j=0}^n, p_{ij} = \begin{cases} 1,\ i = 0, j = 0 \\ 0,\ i < j \\ 2\left(\frac{2}{L} p_{i-1,j-1} - p_{i-1,j}\right) - p_{i-2,j}, i \geq j, i, j \neq 0 \end{cases}$

where A_n is full rank and invertible.

4.2. Approximation of unknown function

For any continuous function of one variable $v(x) \in L^2([0, L])$, it can be approximated by the shifted Chebyshev wavelet function.

$$v(x) = \sum_{i=0}^{\infty} c_i G_i(x) \tag{19}$$

where c_i is the coefficient of shifted Chebyshev wavelet function. The orthogonality of the shifted Chebyshev wavelet function is used to get

$$c_i = \frac{1}{h_i} \int_0^L v(x) G_i(x) v_L(x) dx, i = 0, 1, 2, \cdots$$

A finite number of terms are truncated, the function could be written as

$$v(x) \approx \sum_{i=0}^{n} c_i G_i(x) = C^T \Phi(x), \tag{20}$$

where n is the number of terms of the Chebyshev wavelet function, $C^T = [c_i]_{i=0}^n, \Phi(x) = [G_0(x), G_1(x), \cdots, G_n(x)]^T$.

Any continuous function of two variables $v(x,t) \in L^2([0, L] \times [0, T])$ based on the shifted Chebyshev wavelet function can be approximated

$$v(x,t) = \sum_{i=0}^{\infty} \sum_{j=0}^{\infty} v_{ij} G_i(x) G_j(t), \tag{21}$$

where $v_{ij} = \frac{1}{h_i h_j} \int_0^L \int_0^T v(x,t) G_i(x) G_j(t) v_L(x) v_T(t) dt dx, i, j = 0, 1, 2 \cdots$.

A finite number of terms are truncated, the function could be obtained

$$v(x,t) \approx \sum_{i=0}^{n}\sum_{j=0}^{n} v_{ij} G_i(x) G_j(t) = \Phi^T(x) V \Phi(t) \tag{22}$$

where $\Phi(x) = [G_0(x), G_1(x), \cdots, G_n(x)]^T; \Phi(t) = [G_0(t), G_1(t), \cdots, G_n(t)]^T$, $V = [v_{ij}]_{i,j=0}^{n}$ is the coefficient matrix.

If $v(x,t) \notin L^2([0,L] \times [0,T])$ but belongs to the continuous function space, according to the function approximation theory, the effect of the function approximation will be better. Therefore, the shifted Chebyshev wavelet function may be applied in multivariate fractional calculus.

4.3. Determination of operator matrix

4.3.1. Integer order operator matrix

Definition 2 *If there is a matrix P_x such that $\Phi'(x) = P_x \Phi(x)$, then P_x is called the first order operator matrix of shifted Chebyshev wavelet function.*

$$\begin{aligned} \Phi'(x) &= (A_X Z(x))' = A_X Z'(x) \\ &= A_X \begin{bmatrix} 1' \\ x' \\ \vdots \\ (x^n)' \end{bmatrix} = A_X \begin{bmatrix} 0 \\ 1 \\ \vdots \\ nx^{n-1} \end{bmatrix} = A_X M Z(x) \end{aligned} \tag{23}$$

where A_X is obtained by replacing n by X in Eq. (18),
and

$$M = [m_{ij}]_{i,j=0}^{n}, m_{ij} = \begin{cases} 0, i \neq j+1 \\ i, i = j+1 \end{cases}$$

Because of $Z(x) = A_X^{-1} \Phi(x)$, then the Eq. (23) can be written as

$$\Phi'(x) = A_X M A_X^{-1} \Phi(x) = P_x \Phi(x) \tag{24}$$

where $P_x = A_X M A_X^{-1}$ is a matrix of first order differential operator for shifted Chebyshev wavelet function.

Definition 3 *If there is a matrix G_x such that $\Phi''(x) = G_x \Phi(x)$, then G_x is called the second order operator matrix of shifted Chebyshev wavelet function.*

$$\begin{aligned}\Phi''(x) &= (\Phi'(x))' = \left(A_X M A_X^{-1}\Phi(x)\right)' = A_X M A_X^{-1}\Phi'(x) \\ &= \left(A_X M A_X^{-1}\right)\left(A_X M A_X^{-1}\right)\Phi(x) = (P_x)^2\Phi(x) = G_x\Phi(x) \quad (25)\end{aligned}$$

where $G_x = (P_x)^2 = \left(A_X M A_X^{-1}\right)^2$ is a matrix of second order differential operator for shifted Chebyshev wavelet function.

Based on the derivative of first and second order differential operator matrices, the integer order differential operator matrix of the shifted Chebyshev wavelet function can be expressed as

$$P_x^m = \left(A_X M A_X^{-1}\right)^m \quad (26)$$

where $m \in Z$.

The integer order differential of $\Phi(x)$ can be expressed as

$$\frac{d^m\Phi(x)}{dx^m} = P_x^m\Phi(x) = \left(A_X M A_X^{-1}\right)^m\Phi(x) \quad (27)$$

The partial differential equation terms in Eq. (12) could be obtained:

$$\begin{aligned}\frac{\partial^2 v(x,t)}{\partial x^2} &\approx \frac{\partial^2\left(\Phi^T(x)V\Phi(t)\right)}{\partial x^2} = \frac{\partial^2\Phi^T(x)}{\partial x^2}V\Phi(t) \\ &= \Phi^T(x)\left(P_x{}^T\right)^2 V\Phi(t) = \Phi^T(x)\left(A_X M A_X^{-1}\right)^2 V\Phi(t) \quad (28)\end{aligned}$$

$$\begin{aligned}\frac{\partial^4 v(x,t)}{\partial x^4} &\approx \frac{\partial^4\left(\Phi^T(x)V\Phi(t)\right)}{\partial x^4} = \frac{\partial^4\Phi^T(x)}{\partial x^4}V\Phi(t) \\ &= \Phi^T(x)\left(P_x{}^T\right)^4 V\Phi(t) = \Phi^T(x)\left(A_X M A_X^{-1}\right)^4 V\Phi(t) \quad (29)\end{aligned}$$

$$\begin{aligned}\frac{\partial v(x,t)}{\partial t} &\approx \frac{\partial\left(\Phi^T(x)V\Phi(t)\right)}{\partial t} = \Phi(x)V\frac{\partial\Phi(t)}{\partial t} \\ &= \Phi^T(x)VP_t\Phi(t) = \Phi^T(x)V\left(A_T M A_T^{-1}\right)\Phi(t) \quad (30)\end{aligned}$$

$$\begin{aligned}\frac{\partial^2 v(x,t)}{\partial t^2} &\approx \frac{\partial^2\left(\Phi^T(x)V\Phi(t)\right)}{\partial t^2} = \Phi(x)V\frac{\partial^2\Phi(t)}{\partial t^2} \\ &= \Phi^T(x)V(P_t)^2\Phi(t) = \Phi^T(x)V\left(A_T M A_T^{-1}\right)^2\Phi(t) \quad (31)\end{aligned}$$

4.3.2. Fractional order operator matrix

Definition 4 *If there is a matrix Q_t, such that ${}^cD_t^\alpha \Phi(t) = Q_t \Phi(t)$, then Q_t is called the fractional order operator matrix of shifted Chebyshev wavelet function.*

Based on the definition of the Caputo fractional derivative

$$ {}^cD_t^\alpha t^n = \frac{\Gamma(n+1)}{\Gamma(n+1-\alpha)} t^{n-\alpha} $$

so fractional derivative of $\Phi(t)$ can be written as

$$ \begin{aligned} {}^cD_t^\alpha \Phi(t) &= {}^cD_t^\alpha (A_T Z(t)) = A_T {}^cD_t^\alpha Z(t) = A_T {}^cD_t^\alpha \begin{bmatrix} 1 \\ t \\ \vdots \\ t^n \end{bmatrix} \\ &= A_T \begin{bmatrix} 0 \\ \frac{\Gamma(2)}{\Gamma(2-\alpha)} t^{1-\alpha} \\ \vdots \\ \frac{\Gamma(n+1)}{\Gamma(n+1-\alpha)} t^{n-\alpha} \end{bmatrix} = A_T E Z(t) \end{aligned} \tag{32} $$

where A_T is obtained by replacing n by T in Eq. (18), and

$$ E = [e_{ij}]_{i,j=0}^{n}, e_{ij} = \begin{cases} \frac{\Gamma(i)}{\Gamma(i+1)} t^{-\alpha}, i = j, i \neq 1 \\ 0, otherwise \end{cases} $$

Because of $Z(t) = A_T^{-1} \Phi(t)$, then the Eq. (32) can be written as

$$ {}^cD_t^\alpha \Phi(t) = A_T E A_T^{-1} \Phi(t) = Q_t \Phi(t) \tag{33} $$

where $Q_t = A_T E A_T^{-1}$ is the fractional differential operator matrix of shifted Chebyshev wavelet function.

The fractional partial differential equation term in Eq. (12) could be obtained:

$$ \begin{aligned} {}^cD_t^\alpha \frac{\partial^4 v(x,t)}{\partial x^4} &\approx {}^cD_t^\alpha \Phi^T(x) \left(A_X M A_X^{-1}\right)^4 V \Phi(t) \\ &= \Phi^T(x) \left(A_X M A_X^{-1}\right)^4 V {}^cD_t^\alpha \Phi(t) \\ &= \Phi^T(x) \left(A_X M A_X^{-1}\right)^4 V A_T E A_T^{-1} \Phi(t) \end{aligned} \tag{34} $$

4.4. Discretisation of the governing equation of viscoelastic column

Eq. (12) could be converted into the following form:

$$\begin{aligned}&\rho A\Phi^T(x)V\left(A_TMA_T^{-1}\right)^2\Phi(t)+\beta_0\Phi^T(x)V\left(A_TMA_T^{-1}\right)\Phi(t)\\&+E_0I\Phi^T(x)\left(A_XMA_X^{-1}\right)^4V\Phi(t)+I\eta\Phi^T(x)\left(A_XMA_X^{-1}\right)^4VA_TEA_T^{-1}\Phi(t)\\&+F(t)\Phi^T(x)\left(A_XMA_X^{-1}\right)^2V\Phi(t)=0\end{aligned} \tag{35}$$

Based on the collection method, the reasonable match points $x_i = \frac{2i-1}{2(n+1)}L, i = 1,2,\cdots,n$, $t_j = \frac{2j-1}{2(n+1)}T, j = 1,2,\cdots,n$ are used to discretize the variable (x,t) to (x_i,t_j). Eq. (35) is transformed into a set of algebraic equations.

The coefficient $v_{ij}\,(i=0,1,2,\cdots,n;j=0,1,2,\cdots,n)$ is determined by using Matlab platform and least square method. The numerical solution of the fractional derivative equation can be obtained.

The proposed algorithm can be summarized as shown in Table. 2.

Table 2: Numerical algorithm to resolve the fractional governing equation.

Input:	$n,\ \alpha, E_0, \beta_0, \eta, l, \rho, A, I, F(t)$
Output:	
1.	Function approximation $v(x,t) \approx \Phi^T(x)V\Phi(t)$
2.	Derive the operator matrix of $\Phi(x)$ and $\Phi(t)$ in Eq. 24 and 33.
3.	Substitute Eq. 28 - 31 and Eq. 34 into Eq. 12.
4.	Eq. 12 could be converted into Eq. 35
5.	Let $x_i = \frac{2i-1}{2(n+1)}L, i = 1,2,\cdots,n$, $t_j = \frac{2j-1}{2(n+1)}T, j = 1,2,\cdots,n$
6.	Solve algebraic equations with MATLAB mathematical software
7.	Obtain the solution of the initial equation $v(x,t)$

5. Convergence analysis and validation

In this section, the convergence analysis and numerical example are given to prove the validity and accuracy of the proposed algorithm in solving fractional order equations. The fractional equation solved in section 5.2 is a mathematical example with known algebraic solution. The obtained numerical solutions are compared with the algebraic solution to confirm the efficiency of the proposed algorithm.

5.1. Convergence analysis

In the domain $\Lambda = [0, L] \times [0, \mathrm{T}]$, the norm of any continuous function $v(x,t)$ is

$$\|v(x,t)\| = \sup_{(x,t)\in\Lambda} |v(x,t)| \tag{36}$$

The absolute error is defined as

$$|e_n(x,t)| = |v(x,t) - v_n(x,t)| \tag{37}$$

where $v(x,t)$ and $v_n(x,t)$ are the algebraic and numerical solutions of fractional governing equation of viscoelastic column.

Theorem 1 *If $v(x,t) \in C^3(\Lambda)$, the absolute error bound is*

$$\|e_n(x,t)\| = \|v(x,t) - v_n(x,t)\| \leq Nh^3 = O\left(h^3\right) \tag{38}$$

Proof 1 *Let*

$$e_{n,ij}(x,t) = \begin{cases} v(x,t) - v_n(x,t), (x,t) \in \Lambda_n \\ 0, \qquad\qquad\quad (x,t) \in \Lambda - \Lambda_n \end{cases} \tag{39}$$

where $\Lambda_n = \{(x,t) | ih \leq x < (i+2)h, jh \leq t < (j+2)h, i, j = 0, 2, \cdots, n-2\}$, $v_n(x,t)$ is the quadratic polynomials interpolation function of $v(x,t)$ on Λ_n, then

$$\begin{aligned} e_{n,ij}(x,t) &= \frac{1}{6}\frac{\partial^3 v(\xi_{1,i},t)}{\partial x^3}\prod_{i'=i}^{i+2}(x - x_{i'}) + \frac{1}{6}\frac{\partial^3 v(x,\zeta_{1,j})}{\partial t^3}\prod_{j'=j}^{j+2}(t - t_{j'}) \\ &- \frac{1}{36}\frac{\partial^6 v(\xi_{2,i},\zeta_{2,j})}{\partial x^3 t^3}\prod_{i'=i}^{i+2}(x - x_{i'})\prod_{j'=j}^{j+2}(t - t_{j'}) \end{aligned} \tag{40}$$

where $x, \xi_{1,i}, \xi_{2,i} \in [x_i, x_{i+2}), t, \zeta_{1,j}, \zeta_{2,j} \in [t_j, t_{j+2}), i, j = 0, 2, \cdots, n-2$.

Thus the expression can get

$$\begin{aligned} \|e_{n,ij}(x,t)\| &\leq \frac{1}{6}\left\|\frac{\partial^3 v(\xi_{1,i},t)}{\partial x^3}\right\|\left\|\prod_{i'=i}^{i+2}(x - x_{i'})\right\| \\ &+ \frac{1}{6}\left\|\frac{\partial^3 v(x,\zeta_{1,j})}{\partial t^3}\right\|\left\|\prod_{j'=j}^{j+2}(t - t_{j'})\right\| \\ &+ \frac{1}{36}\left\|\frac{\partial^6 v(\xi_{2,i},\zeta_{2,j})}{\partial x^3 t^3}\right\|\left\|\prod_{i'=i}^{i+2}(x - x_{i'})\right\|\left\|\prod_{j'=j}^{j+2}(t - t_{j'})\right\| \end{aligned} \tag{41}$$

where $\left\|\prod_{i'=i}^{i+2}(x-x_{i'})\right\| = \sup_{x\in[x_i,x_{i+2})}\left|\prod_{i'=i}^{i+2}(x-x_{i'})\right|$.

Based on the maximum value of $\left|\prod_{i'=i}^{i+2}(x-x_{i'})\right|$ *in* $x=\left(i+1-\frac{\sqrt{3}}{3}\right)h$, *the following expression could be obtained*

$$\left\|\prod_{i'=i}^{i+2}(x-x_{i'})\right\| \leq \frac{2\sqrt{3}h^3}{9}, \forall x\in[x_i,x_{i+2}) \tag{42}$$

$$\left\|\prod_{j'=j}^{j+2}(t-t_{j'})\right\| \leq \frac{2\sqrt{3}h^3}{9}, \forall t\in[t_j,t_{j+2}) \tag{43}$$

Substituting Eq. (42) and (43) into the Eq. (41) to obtain:

$$\begin{aligned}\|e_n(x,t)\| &\leq \frac{\sqrt{3}h^3}{27}\left(\left\|\frac{\partial^3 v(x,t)}{\partial x^3}\right\| + \left\|\frac{\partial^3 v(x,t)}{\partial t^3}\right\| + \frac{\sqrt{3}h^3}{27}\left\|\frac{\partial^6 v(x,t)}{\partial x^3\partial t^3}\right\|\right)\\ &= Nh^3 = O(h^3)\end{aligned} \tag{44}$$

As conclusion, the theorem is proved.

Based on the proof of the theorem, the accuracy of the proposed algorithm is confirmed and it can used to solve the fractional order equations effectively.

5.2. Application of developed algorithm for solving mathematical problem

The objective of this section is to investigate the accuracy of the proposed numerical algorithm.

The order of convergence is calculated to describe the effectiveness of the proposed numerical algorithm. The order of convergence q is expressed as follows:

$$q = \frac{\log\left(\frac{e^n_{\max}}{e^{n-1}_{\max}}\right)}{\log\left(\frac{h_n}{h_{n-1}}\right)} \tag{45}$$

where $e^n_{\max}$ and $e^{n-1}_{\max}$ are the maximum absolute error, $h_n = \frac{\pi}{2n}$, $h_{n-1} = \frac{\pi}{2(n-1)}$.

The following equation is considered as a numerical example:

$$50\frac{\partial^2 v\left(x,t\right)}{\partial t^2}+1.6\frac{\partial v\left(x,t\right)}{\partial t}+0.15\frac{\partial^4 v\left(x,t\right)}{\partial x^4}+0.15D_t^{\alpha}\frac{\partial^4 v\left(x,t\right)}{\partial x^4}$$
$$+0.1F\left(x,t\right)\frac{\partial^2 v\left(x,t\right)}{\partial x^2}=0 \tag{46}$$

The boundary and initial conditions are:

$$\begin{cases} v\left(0,t\right)=v\left(5,t\right)=0 \\ v'\left(0,t\right)=v'\left(5,t\right)=0 \\ v\left(x,0\right)=v'\left(x,0\right)=0 \end{cases} \tag{47}$$

where $\alpha=0.89, F\left(x,t\right)=\frac{x^2(5-x)^2(100+3.2t)+3.6\left(t^2+\frac{\Gamma(3)}{\Gamma(2.11)}t^{1.11}\right)}{(6x-1.2x^2-5)t^2}$.

The algebraic solution of the Eq. (46) is $v\left(x,t\right)=\frac{x^2(5-x)^2t^2}{145}$.

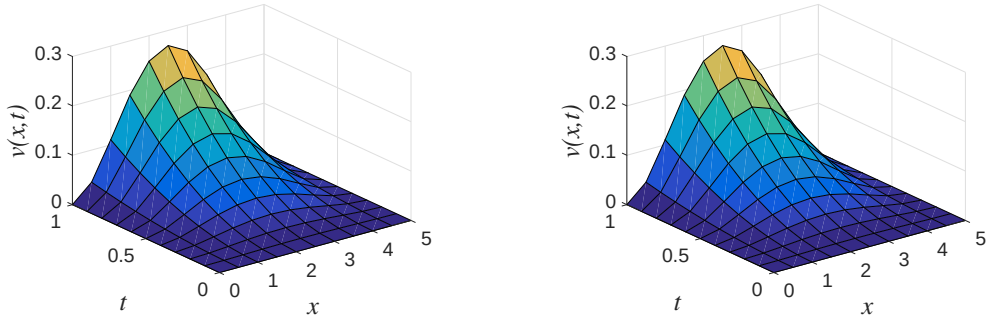

(a) algebraic solution (b) numerical solution

Figure 3: The comparison of the numerical and algebraic solutions at different matching point when $n=5$.

The numerical solution of the equation is obtained with different number of terms of the shifted Chebyshev wavelet function ($n=4, n=5$ and $n=6$) based on the proposed algorithm at $(x_i,t_j)\in[0,5]\times[0,1]$. The numerical solution is highly consistent with the algebraic solution, as shown in Figure. 3 ($n=5$). The absolute error values between the numerical and algebraic solutions at different matching points are listed in Table. 3. The maximum absolute error value and order of convergence of different n are shown in Table. 4.

The absolute error, defined in Eq. (37), between the numerical and algebraic solutions decreases gradually with the number of terms of shifted

Table 3: Evolution of absolute error using the developed method in function of several values of n.

(x,t)	Algebraic solution	Absolute error value		
		$n=4$	$n=5$	$n=6$
$(0,0)$	0	1.182×10^{-8}	7.567×10^{-10}	1.284×10^{-11}
$(0,0.5)$	0	3.966×10^{-9}	2.259×10^{-10}	1.19×10^{-12}
$(0,1)$	0	1.02×10^{-8}	6.515×10^{-10}	1.988×10^{-11}
$(2.5,0)$	0	3.766×10^{-9}	5.163×10^{-10}	1.258×10^{-11}
$(2.5,0.5)$	0.06735	5.856×10^{-6}	3.29×10^{-7}	5.841×10^{-9}
$(2.5,1)$	0.2694	1.168×10^{-5}	6.557×10^{-7}	1.162×10^{-8}
$(4,0)$	0	4.726×10^{-9}	6.988×10^{-10}	1.872×10^{-11}
$(4,0.5)$	0.02759	2.236×10^{-6}	1.251×10^{-7}	2.225×10^{-9}
$(4,1)$	0.1103	4.462×10^{-6}	2.498×10^{-7}	4.436×10^{-9}

Table 4: The maximum absolute error value and order of convergence for different n.

n	$e^n_{\max}$	q
3	1.196×10^{-4}	–
4	1.168×10^{-5}	71.9530
5	6.557×10^{-7}	136.6654
6	1.162×10^{-8}	199.0116

Chebyshev wavelet functions. The order of convergence is improved with the increase of the number of terms. The efficiency and accuracy of the proposed algorithm based on the shifted Chebyshev wavelet function is demonstrated. Therefore, $n = 6$ is retained in the numerical algorithm for the following solutions. It is proved as a highly useful method to solve the fractional governing equation of the viscoelastic column under various load conditions.

6. Results and discussions

The actual fractional governing equation of the viscoelastic column is solved by using the proposed algorithm.

The displacement, stress and strain of the viscoelastic columns with different cross-section shape and materials under various load conditions are investigated in this section. The square and circular cross-section parameters are shown in Table. 5.

The boundary and initial conditions are as following:

$$v\left(0,t\right)=v\left(l,t\right)=0,\frac{\partial v\left(0,t\right)}{\partial x}=\frac{\partial v\left(l,t\right)}{\partial x}=0 \tag{48}$$

Table 5: Square and circular cross-section parameters of viscoelastic column.

	d(m)	A(m^2)	I(m^4)
square cross-section	0.1	0.01	8.3×10^{-6}
circular cross-section	0.1128	0.01	8.03×10^{-6}

$$v\left(x,0\right)=\frac{\partial v\left(x,0\right)}{\partial t}=0. \tag{49}$$

6.1. Effect of the load condition on the numerical solution of governing equation

6.1.1. Axial compressive force

The column with the square cross-section is selected in this study. The metal material parameters of the viscoelastic properties are defined in Table. 1. When the axial compression force 1000 N is applied on the column and the numerical solutions of the displacement of the column at various position and time are shown in Figure. 4.

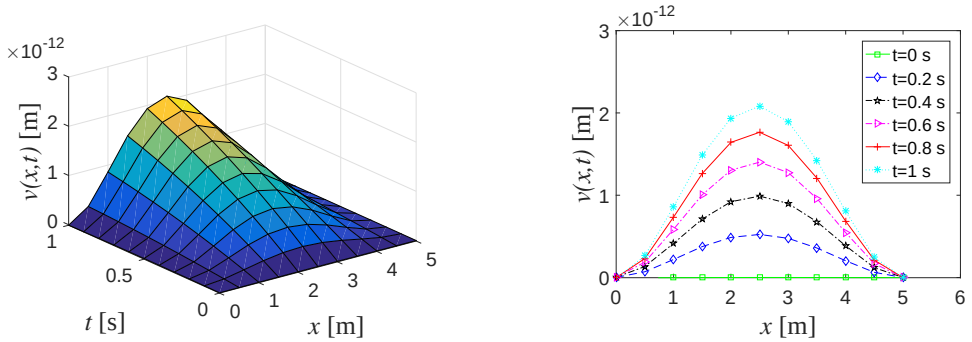

(a) F = 1000 N (b) At different times

Figure 4: The displacement solution of viscoelastic column under axial compressive force: (a) F = 1000 N, (b) at different times.

The displacement of the two ends of a viscoelastic column is always zero and is not affected by time, which is coherent with the boundary conditions. In other locations, the displacement of the viscoelastic column gradually increases with time and the maximum value is obtained at $t = 1$ s. The maximum transverse displacement of the viscoelastic column is obtained at

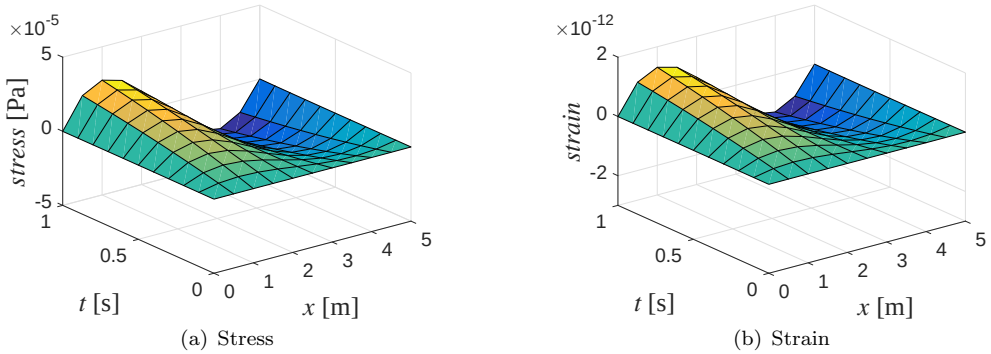

(a) Stress (b) Strain

Figure 5: Evolution of (a) stress (Pa) and (b) strain of viscoelastic column under the axial compressive force.

the middle of the column $x = 2.5$ m. The displacement of the column is symmetrical to the middle of the column.

Based on the constitutive relation of the viscoelastic material, the distribution of stress and strain of the viscoelastic column under axial compressive force are shown in Figure. 5. The stress curves and strain curves of the column exhibit the same trend in function of time and position. The stress and strain values at both ends of the column are zero during the whole loading process. The stress and strain values at $t = 0$ s are zero, which is coherent with the initial conditions. The strain value at $x = 2.5$ m is zero because no deformation occurs at the midpoint of the column, which results in the zero stress at the same position. The strain curves are symmetrical to the midpoint of the column and the maximum absolute value of the strain is obtained at $x = 1.25$ m and $x = 3.75$ m.

The numerical solutions of the transverse displacement of the viscoelastic column under different loads conditions are obtained in the time domain, which are shown in Figure. 6. The displacement of the viscoelastic column increases gradually with time. The maximum transverse displacement is approximately 2×10^{-12} m under the applied compressive force of 1000 N, as shown in Figure. 4(a). It becomes 1×10^{-6} m under 1500 N and 2×10^{-6} m under 2000 N. The transverse displacement increases with the applied axial compressive force.

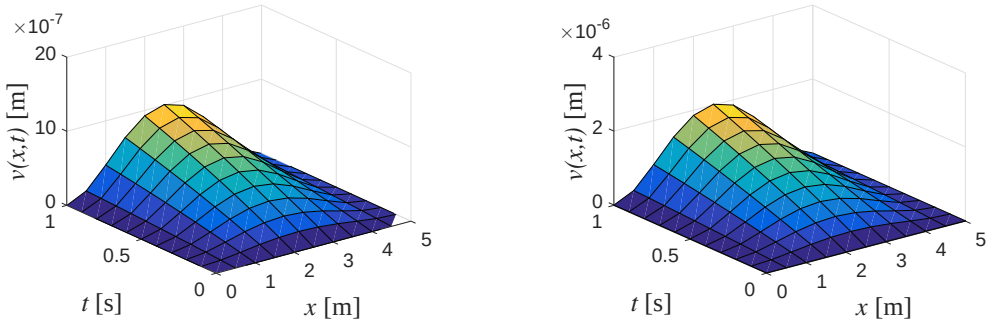

(a) F = 1500 N (b) F = 2000 N

Figure 6: The numerical solution of displacement under different load conditions: (a) F = 1500 N, (b) F = 2000 N.

6.1.2. Harmonic load

A harmonic load $F = B\cos(\omega\pi t)$ is applied on the viscoelastic column. The transverse displacement of the viscoelastic column is obtained with different value of B and ω, as shown in Figure. 7. The transverse displacement of the column is affected by the value of B and ω have effects on the transverse displacement of the column. The transverse displacement of the column decreases with the value of ω, as shown in Figures. 7(a), 7(b), 7(c). The transverse displacement of the viscoelastic column decreases gradually when the period of the applied harmonic load becomes smaller. The transverse displacement of the column increases with the value of B, as shown in Figures. 7(a), 7(d).

The displacement of the fractional viscoelastic column under the periodic load was analyzed by Li et al. [46]. Therefore, the proposed algorithm was limited to a specific displacement solution. The algorithm used in this paper exhibits wider application and higher efficiency.

6.2. Effect of the column cross-section on the numerical solution of governing equation

The effect of cross-section parameters on the transverse displacement of the viscoelastic column is investigated in this section. Two viscoelastic columns with different cross-section shape (square and circular) are retained in this study. Their cross-sectional areas are the same and the cross-section parameters are summarized in Table. 5. The transverse displacement of the viscoelastic column with circular cross-section shape under the axial

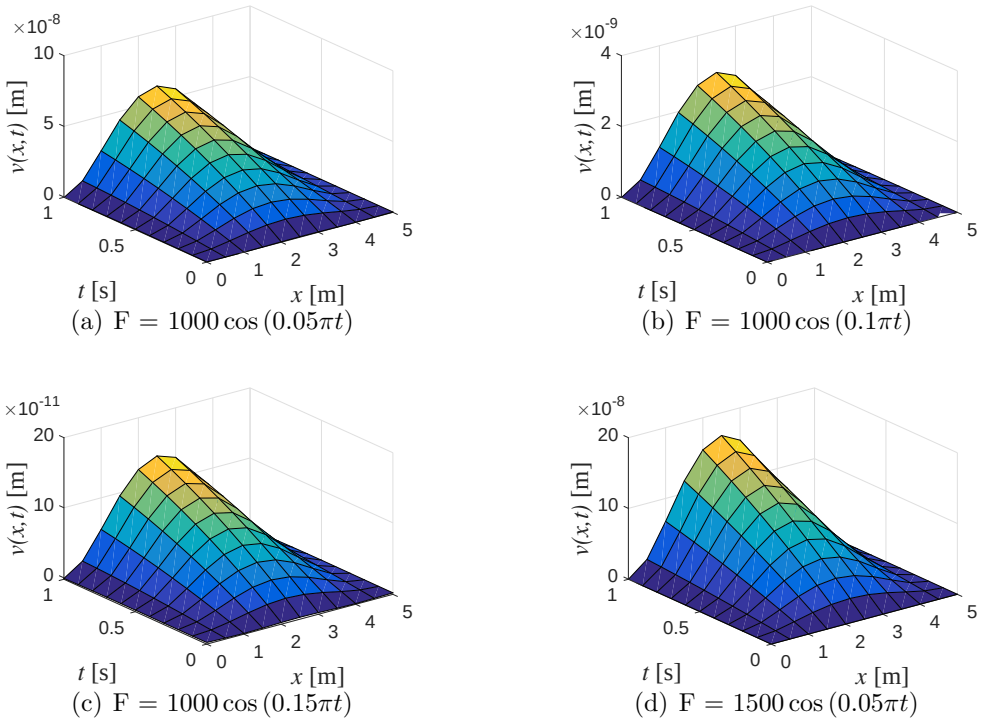

(a) F = 1000 cos (0.05πt) (b) F = 1000 cos (0.1πt)

(c) F = 1000 cos (0.15πt) (d) F = 1500 cos (0.05πt)

Figure 7: Transverse displacement of viscoelastic column under different harmonic loads: (a) F = 1000 cos (0.05πt), (b) F = 1000 cos (0.1πt), (c) F = 1000 cos (0.15πt), (d) F = 1500 cos (0.05πt)

compressive force of 1000 N is shown in Figure. 8.

Based on the comparison between Figures. 4 and 8, the evolution of the transverse displacement of the column with square and circular cross-section is similar. However, the transverse displacement of the column with circular cross-section is smaller than that with square cross-section, when the columns exhibit the same cross-sectional area and are under the same axial compressive load condition.

6.3. Effect of material property on the numerical solution of governing equation

The deformation of the viscoelastic columns with two different materials (concrete and polymer) are compared in this part. The material parameters are summarized in Table. 1. The viscoelastic columns exhibit the same

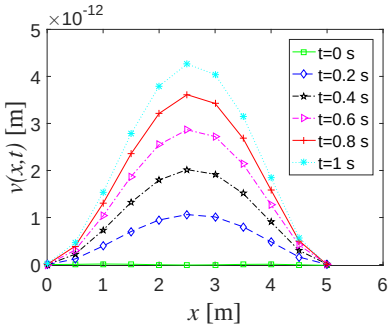

Figure 8: Displacement of a viscoelastic column with circular cross-section at different times.

square cross-section and subjected the same applied compressive force 1000 N. The proposed algorithm based on the shifted Chebyshev wavelet function is used to calculate the transverse displacement of the viscoelastic column. The maximum value of the transverse displacement of concrete column is approximately 1.913×10^{-10} m, however, the maximum value of the transverse displacement of polymer column is approximately 8.352×10^{-4} m. The maximum value of transverse displacement of polymer column is larger than that of the concrete column.

The stress and strain curves of the viscoelastic columns with polymer and concrete material in function of position and time are shown in Figures. 9 and 10. The stress and strain are calculated according to Eqs. (5) and (8). The trend of the stress and strain curves is similar with different materials. Therefore, the values of stress and strain of polymer column are extremely larger than those of the concrete column. The maximum value of the strain in polymer column is approximately 5×10^{-4}, when the maximum value of the strain in concrete column is approximately 1×10^{-10}. The maximum value of the stress in polymer column is approximately 1900 Pa, when the maximum value of the stress in concrete column is approximately 2.5×10^{-3} Pa. This is mainly due to the smaller value of elastic modulus of the polymeric material.

7. Conclusions

In this paper, a numerical algorithm based on the shifted Chebyshev wavelet function is developed to solve the fractional governing equation of the viscoelastic column directly in the time domain. The fractional derivative model is used to describe the viscoelastic behaviour of the column

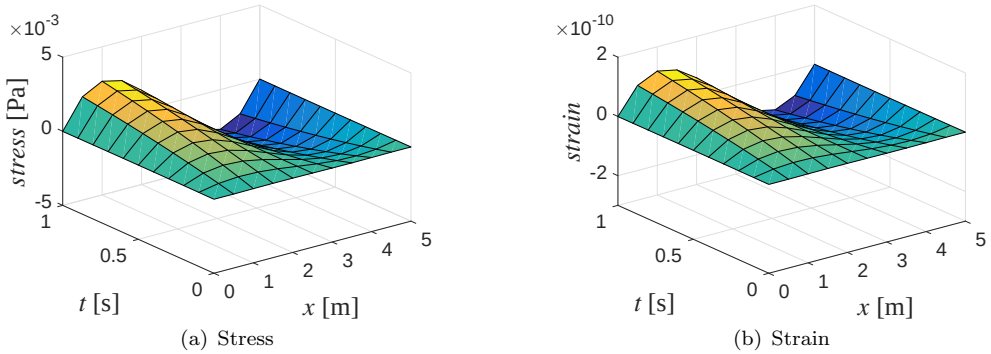

(a) Stress (b) Strain

Figure 9: Stress and strain of concrete viscoelastic column.

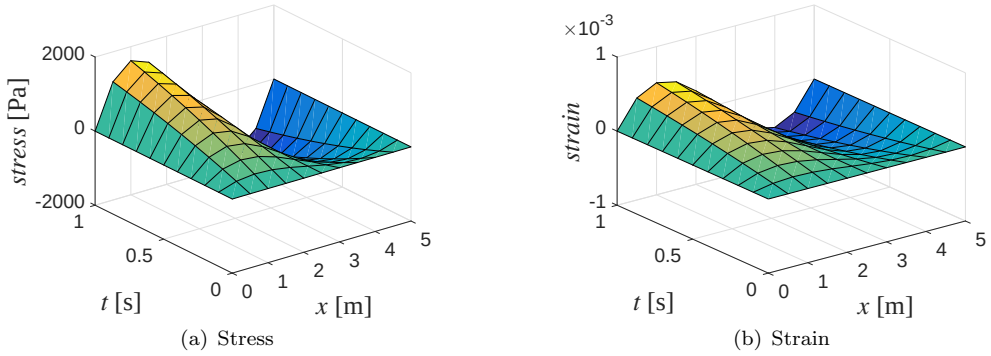

(a) Stress (b) Strain

Figure 10: Stress and strain of polymer viscoelastic column.

with different materials. The transverse displacement, stress and strain of the viscoelastic column are obtained under various load conditions: axial compressive force and harmonic load.

1. Base on the analysis of the mathematical example, it is proved that the proposed algorithm exhibits high accuracy in solving the fractional order equations. The accuracy of the algorithm improves with the number of terms retained in the shifted Chebyshev wavelet function.

2. The transverse displacement of viscoelastic column under axial compressive force and harmonic load are obtained. The displacement increases with the applied axial compression force. The magnitude and period of the harmonic load affects the deformation of the viscoelastic column.

3. The transverse displacement of the viscoelastic column with circular

cross-section shape is smaller than that with square cross-section, when the columns exhibit the same cross-sectional area and are under the same axial compressive force.

4. The polymer column exhibits the larger displacement than the concrete column, due to its lower elastic modulus. The proposed algorithm demonstrates good sensitivity of material in the numerical simulation of the deformation of the viscoelastic column.

Acknowledgements

This work is supported by the Natural Science Foundation of Hebei Province (A2017203100) in China and the EIPHI Graduate School (contract ANR-17-EURE-0002).

Symbol description

symbol	explanation
α	fractional order
${}^{c}D_{t}^{\alpha}$	Caputo fractional derivative operator
$f(t)$	continuous function
$\Gamma(\cdot)$	Gamma function
C	constant
FZM	Four-parameter Zener model
PTM	Poynting-Thomson model
FMM	Fractional Maxwell model
FKVM	Fractional Kelvin-Voigt model
x, z	coordinates
t	time in s
l	height of viscoelastic column in m
$\sigma(x,t)$	stress in Pa
$\varepsilon(x,t)$	strain
$v(x,t)$	transverse displacement in m
E_0	elastic modulus in MPa
ρ	density in kg/m^3
β_0	damping coefficient
η	viscosity
A	cross-sectional area in m^2

d	diameter in m
I	moment of inertia in m^4
$M(x,t)$	bending moment
$F(t)$	axial compressive load in N
T_i, T_{i+1}, T_{i-1}	Chebyshev polynomials
G_i, G_{i+1}, G_{i-1}	shifted Chebyshev wavelet function
$\Phi(x), \Phi(t)$	shifted Chebyshev wavelet function matrix
n	number of terms of shifted Chebyshev wavelet function
$Z(x), Z(t)$	basis function
A_n, A_X, A_T	coefficients of Chebyshev wavelet function matrix
P_x	first order differential operator matrix for x
G_x	second order differential operator matrix for x
P_x^m	m^{th} order differential operator matrix for x
Q_t	fractional differential operator matrix for t
v_n	numerical solution
e_n	error
$\|e_n(x,t)\|$	absolute error
$e_{\max}^n$	maximum absolute error
q	order of convergence

Reference

References

[1] J.T. Machado, Fractional order generalized information, Entropy. 16 (2014) 2350−2361. https://doi.org/10.3390/e16042350.

[2] J. Xu, Y.D. Chen, Y.P. Tai, X.M. Xu, G.D. Shi, N. Chen, Vibration analysis of complex fractional viscoelastic beam structures by the wave method, Int. J. Mech. Sci. 167 (2020) 105204. https://doi.org/10.1016/j.ijmecsci.2019.105204.

[3] J. Mendiguren, F. Cortés, L. Galdos, A generalised fractional derivative model to represent elastoplastic behaviour of metals, Int. J. Mech. Sci. 65 (2012) 12−17. https://doi.org/10.1016/j.ijmecsci.2012.08.008.

[4] H. Sherief, A.M. Abd El-Latief, Effect of variable thermal conductivity on a half-space under the fractional order theory of thermoelasticity, Int. J. Mech. Sci. 74 (2013) 185−189. https://doi.org/10.1016/j.ijmecsci.2013.05.016.

[5] B.L. Konstantinos, A.P. Athanasios, A.K. Ioannis, T.M. Antonios, P. Antonina, Implicit analytic solutions for a nonlinear fractional partial differential beam equation, Commun. Nonlinear. Sci. Numer. Simulat. 85 (2020) 105219. https://doi.org/10.1016/j.cnsns.2020.105219.

[6] L. Liu, L.C. Zheng, Y.P. Chen, F.W. Lin, Fractional boundary layer flow and heat transfer over a stretching sheet with variable thickness, J. Heat. Tran. 140 (2018) 091701.1−091701.9. https://doi.org/10.1115/1.4039765.

[7] Q. Ling, X.L. Jin, Z.L. Huang, Response and stability of SDOF viscoelastic system under wideband noise excitations, J. Franklin. I. 348 (2011) 2026−2043. https://doi.org/10.1016/j.jfranklin.2011.05.019.

[8] G. Aman, C.O. Arun, Stochastic meshfree method for elastic buckling analysis of columns, Comput. Struct. 194 (2018) 32−47. https://doi.org/10.1016/j.compstruc.2017.08.014.

[9] M. Jin, An analysis of dynamic stability of an elastic column, Theor. Appl. Mech. Lett. 8 (2018) 68−74. https://doi.org/10.1016/j.taml.2018.02.002.

[10] Jones, I.G. David, Handbook of viscoelastic vibration damping, Wiley, New York, 2001.

[11] H.T. Yang, Z. Han, Y.Q. He, Numerical analysis of static and dynamic stabilities of viscoelastic columns, Math. Meth. Appl. Sci. 39 (2016) 3932−3946. https://doi.org/10.1002/mma.3786.

[12] J. Deng, W.C. Xie, M.D. Pandey, Stochastic stability of a fractional viscoelastic column under bounded noise excitation, J. Sound. Vib. 333 (2014) 1629−1643. https://doi.org/10.1016/j.jsv.2013.11.019.

[13] J. Deng, W.C. Xie, M.D. Pandey, Higher-order stochastic averaging to study stability of a fractional viscoelastic column, J. Sound. Vib. 333 (2014) 6121−6139. https://doi.org/10.1016/j.jsv.2014.06.012.

[14] A. Yadav, S.K. Panda, T. Dey, Non-linear dynamic instability analysis of mono-symmetric thin walled columns with various boundary conditions, Int. J. Mech. Sci. 126 (2017) 242−254. https://doi.org/10.1016/j.ijmecsci.2017.03.035.

[15] C. Floris, Stochastic stability of a viscoelastic column axially loaded by a white noise force, Mech. Res. Commun. 38 (2011) 57−61. https://doi.org/10.1016/j.mechrescom.2010.11.001.

[16] A.Y.T. Leung, H.X. Yang, J.Y. Chen, Parametric bifurcation of a viscoelastic column subject to axial harmonic force and time-delayed control, Comput. Struct. 136 (2014) 47−55. https://doi.org/10.1016/j.compstruc.2014.01.015.

[17] W. Zhang, C. Adela, S. Gerhard, A.H. Gerhard, A.N. David, An efficient and accurate method for modeling nonlinear fractional viscoelastic biomaterials, Comput. Method. Appl. M. 362 (2020) 112834. https://doi.org/10.1016/j.cma.2020.112834.

[18] Y.F. Pu, P. Siarry, J.L. Zhou, A fractional partial differential equation based multiscale denoising model for texture image, Math. Method. Appl. Sci. 37 (2014) 1784−1806. https://doi.org/10.1002/mma.2935.

[19] Y. Wang, L. Mei, Q. Li, Split-step spectral Galerkin method for the two-dimensional nonlinear space-fractional Schrödinger equation, Appl. Numer. Math. 136 (2019) 257−278. https://doi.org/10.1016/j.apnum.2018.10.012.

[20] Z. Yang, Z. Yuan, Y. Nie, Finite element method for nonlinear Riesz space fractional diffusion equations on irregular domains, J. Comput. Phys. 330 (2017) 863−883. https://doi.org/10.1016/j.jcp.2016.10.053.

[21] E.B.H. David, M.G. Nicolás, A numerical method for solving Caputo's and Riemann-Liouville's fractional differential equations which includes multi-order fractional derivatives and variable coefficients, Commun. Nonlinear. Sci. Numer. Simulat. 84 (2020) 105180. https://doi.org/10.1016/j.cnsns.2020.105180.

[22] X.J. Chen, F.H. Zeng, G.E. Karniadakis, A tunable finite difference method for fractional differential equations with non-smooth solutions, Comput. Method. Appl. M. 318 (2017) 193−214. https://doi.org/10.1016/j.cma.2017.01.020.

[23] H.T. Qi, X.W. Guo, Transient fractional heat conduction with generalized Cattaneo model, Int. J. Heat. Mass. Tran. 76 (2014) 535−539. https://doi.org/10.1016/j.ijheatmasstransfer.2013.12.086.

[24] Y.M. Chen, L.Q. Liu, D.Y. Liu, D. Boutat, Numerical study of a class of variable order nonlinear fractional differential equation in terms of Bernstein polynomials, Ain. Shams. Eng. J. 9 (2016) 1235−1241. https://doi.org/10.1016/j.asej.2016.07.002.

[25] B. Yuttanan, M. Razzaghi, Legendre wavelets approach for numerical solutions of distributed order fractional differential equations, Appl. Math. Model. 70 (2019) 350−364. https://doi.org/10.1016/j.apm.2019.01.013.

[26] J. Wang, T.Z. Xu, G.W. Wang, Numerical algorithm for time-fractional Sawada-Kotera equation and Ito equation with Bernstein polynomials, Appl. Math. Comput. 338 (2018) 1−11. https://doi.org/10.1016/j.amc.2018.06.001.

[27] M. Bourne, J.R. Winkler, S. Yi, The computation of the degree of an approximate greatest common divisor of two Bernstein polynomials, Appl. Numer. Math. 111 (2017) 17−35. https://doi.org/10.1016/j.cam.2019.112373.

[28] M.R.A. Sakran, Numerical solutions of integral and integro-differential equations using Chebyshev polynomials of the third kind, Appl. Math. Comput. 351 (2019) 66−82. https://doi.org/10.1016/j.amc.2019.01.030.

[29] S. Foucart, J.B. Lasserre, Computation of Chebyshev polynomials for union of intervals, Comput. Meth. Funct. Th. 19 (2019) 625−641. https://doi.org/10.1007/s40315-019-00285-w.

[30] N.H. Sweilam, A.M. Nagy, A.A. El-Sayed, Second kind shifted Chebyshev polynomials for solving space fractional order diffusion equation, Chaos. Soliton. Fract. 73 (2015) 141−147. https://doi.org/10.1016/j.chaos.2015.01.010.

[31] Y.M. Chen, X.H. Ke, Y.Q. Wei, Numerical algorithm to solve system of nonlinear fractional differential equations based on wavelets method and the error analysis, Appl. Math. Comput. 251 (2015) 475−488. https://doi.org/10.1016/j.amc.2014.11.079.

[32] L.P. Wang, Y.M. Chen, D.Y. Liu, Numerical algorithm to solve generalized fractional pantograph equations with variable coefficients

based on shifted Chebyshev polynomials, Int. J. Comput. Math. 96 (2019) 1−27. https://doi.org/10.1080/00207160.2019.1573992.

[33] C.X. Yu, J. Zhang, Y.M. Chen, Y.J. Feng, A.M. Yang, A numerical method for solving fractional-order viscoelastic Euler-Bernoulli beams, Chaos. Soliton. Fract. 128 (2019) 275−279. https://doi.org/10.1016/j.chaos.2019.07.035.

[34] H. Hassani, M.J.A. Tenreiro, Z. Avazzadeh, E. Naraghirad, Generalized shifted Chebyshev polynomials: Solving a general class of nonlinear variable order fractional PDE, Commun. Nonlinear. Sci. Numer. Simulat. 85 (2020) 105229. https://doi.org/10.1016/j.cnsns.2020.105229.

[35] M. Yi, L. Wang, H. Jun, Legendre wavelets method for the numerical solution of fractional integro-differential equations with weakly singular kernel, Appl. Math. Model. 40 (2016) 3422−3437. https://doi.org/10.1016/j.apm.2015.10.009.

[36] H. Taghvafard, G.H. Erjaee, Phase and anti-phase synchronization of fractional order chaotic systems via active control, Commun. Nonlinear. Sci. 16 (2011) 4079−4088. https://doi.org/10.1016/j.cnsns.2011.02.015.

[37] K. Diethelm, The Analysis of Fractional Differential Equations, Springer, Berlin Heidelberg, 2010.

[38] T. Pritz, Analysis of four-parameter fractional derivative model of real solid materials, J. Sound. Vib. 195 (1996) 103−115. https://doi.org/10.1006/jsvi.1996.0406.

[39] H.Y. Xu, X.Y. Jiang, Creep constitutive models for viscoelastic materials based on fractional derivatives, Comput. Math. Appl. 73 (2017) 1377−1384. https://doi.org/10.1016/j.camwa.2016.05.002.

[40] M. Shen, S.R. Chen, F.W. Liu, Unsteady MHD flow and heat transfer of fractional Maxwell viscoelastic nanofluid with Cattaneo heat flux and different particle shapes, Chinese. J. Phys. 56 (2018) 1199−1211. https://doi.org/10.1016/j.cjph.2018.04.024.

[41] D. Ren, X.Q. Shen, C. Li, X.S. Cao, The fractional Kelvin-Voigt model for Rayleigh surface waves in viscoelastic FGM

infinite half space, Mech. Res. Commun. 87 (2018) 53−58. https://doi.org/10.1016/j.mechrescom.2017.12.004.

[42] L. Liu, F.W. Liu, Boundary layer flow of fractional Maxwell fluid over a stretching sheet with variable thickness, Appl. Math. Lett. 79 (2018) 92−99. https://doi.org/10.1016/j.aml.2017.10.008.

[43] E. Farno, J.C. Baudez, N. Eshtiaghi, Comparison between classical Kelvin-Voigt and fractional derivative Kelvin-Voigt models in prediction of linear viscoelastic behaviour of waste activated sludge, Sci. Total. Environ. 613 (2018) 1031−1036. https://doi.org/10.1016/j.scitotenv.2017.09.206.

[44] R.R. Bellum, K. Muniraj, S.R.C. Madduru, Investigation on modulus of elasticity of fly ash-ground granulated blast furnace slag blended geopolymer concrete, Mater. Today. Process. 27 (2020) 718−723. https://doi.org/10.1016/j.matpr.2019.11.299.

[45] G. Cheng, M. Sahli, J.C. Gelin, T. Barriere, Physical modelling, numerical simulation and experimental investigation of microfluidic devices with amorphous thermoplastic polymers using a hot embossing process, J. Mater. Process. Tech. 229 (2016) 36−53. https://doi.org/10.1016/j.jmatprotec.2015.08.027.

[46] G.G. Li, Z.Y. Zhu, C.Y. Cheng, Dynamical stability of viscoelastic column with fractional derivative constitutive relation, Appl. Math. Mech. 3 (2011) 294−303. https://doi.org/10.1023/A:1015506420053.